AFRL-RY-WP-TP-2013-0165

LONGWAVE-IR OPTICAL PARAMETRIC OSCILLATOR IN ORIENTATION-PATTERNED GaAs PUMPED BY A 2 μm Tm,Ho:YLF LASER (PREPRINT)

Rita Peterson and Ryan Feaver

Optoelectronic Technology Branch
Aerospace Components & Subsystems Division

Peter Powers

University of Dayton

AUGUST 2013
Interim

AIR FORCE RESEARCH LABORATORY
SENSORS DIRECTORATE
WRIGHT-PATTERSON AIR FORCE BASE, OH 45433-7320
AIR FORCE MATERIEL COMMAND
UNITED STATES AIR FORCE

REPORT DOCUMENTATION PAGE

Form Approved
OMB No. 0704-0188

1. REPORT DATE *(DD-MM-YY)*	2. REPORT TYPE	3. DATES COVERED *(From - To)*
August 2013	Journal Article Preprint	1 October 2011 – 15 August 2013

4. TITLE AND SUBTITLE

LONGWAVE-IR OPTICAL PARAMETRIC OSCILLATOR IN ORIENTATION-PATTERNED GaAs PUMPED BY A 2 μm Tm,Ho:YLF LASER (PREPRINT)

5a. CONTRACT NUMBER
In-house

5b. GRANT NUMBER

5c. PROGRAM ELEMENT NUMBER
62204F

6. AUTHOR(S)
Rita Peterson and Ryan Feaver (AFRL/RYDH)
Peter Powers (University of Dayton)

5d. PROJECT NUMBER
2003

5e. TASK NUMBER
11

5f. WORK UNIT NUMBER
Y0EJ

7. PERFORMING ORGANIZATION NAME(S) AND ADDRESS(ES)
Optoelectronic Technology Branch
Aerospace Components & Subsystems Division
Air Force Research Laboratory, Sensors Directorate
Wright-Patterson Air Force Base, OH 45433-7320
Air Force Materiel Command, United States Air Force

University of Dayton
300 College Park Avenue
Dayton, OH 45469

8. PERFORMING ORGANIZATION REPORT NUMBER
AFRL-RY-WP-TP-2013-0165

9. SPONSORING/MONITORING AGENCY NAME(S) AND ADDRESS(ES)
Air Force Research Laboratory , Sensors Directorate
Wright-Patterson Air Force Base, OH 45433-7320
Air Force Materiel Command
United States Air Force

10. SPONSORING/MONITORING AGENCY ACRONYM(S)
AFRL/RYDH

11. SPONSORING/MONITORING AGENCY REPORT NUMBER(S)
AFRL-RY-WP-TP-2013-0165

12. DISTRIBUTION/AVAILABILITY STATEMENT
Approved for public release; distribution unlimited.

13. SUPPLEMENTARY NOTES
Journal article to be submitted to Optical Society of America. ©2013 OSA. The U.S. Government is joint author of the work and has the right to use, modify, reproduce, release, perform, display or disclose the work.PAO Case Number 88ABW-2013-2563, Clearance Date 29 May 2013. Document contains color.

14. ABSTRACT
We demonstrate longwave infrared (LWIR) generation with an optical parametric oscillator (OPO) based on quasi-phasematched orientation-patterned gallium arsenide (OPGaAs). The OPGaAs OPO was directly pumped with a Q-switched λ=2.054 μm Tm,Ho:YLF laser. OPGaAs samples representing three different grating periods were used to explore the LWIR OPO performance yielding outputs ranging from λ=2.5-2.7 μm (signal) and λ=8.8-11.5 μm (idler). Slope efficiencies for the combined signal and idler outputs reach as high as 26% while slope efficiencies for only the idler reached 8%. Spectral measurements of OPO output confirm good agreement with theoretical calculations.

15. SUBJECT TERMS
longwave, infrared, oscillator

16. SECURITY CLASSIFICATION OF:			17. LIMITATION OF ABSTRACT:	18. NUMBER OF PAGES	19a. NAME OF RESPONSIBLE PERSON (Monitor)
a. REPORT	b. ABSTRACT	c. THIS PAGE			Rita Peterson
Unclassified	Unclassified	Unclassified	SAR	10	19b. TELEPHONE NUMBER *(Include Area Code)* N/A

Longwave-IR Optical Parametric Oscillator in Orientation-Patterned GaAs pumped by a 2 μm Tm,Ho:YLF laser

R. K. Feaver,[1,2,*] R. D. Peterson,[1] and P. E. Powers[2]
[1]*Air Force Research Laboratory, 2241 Avionics Cir., Wright-Patterson AFB, OH 45433, USA*
[2]*University of Dayton, 300 College Park Avenue, Dayton, OH 45469, USA*
**Ryan.Feaver@wpafb.af.mil*

Abstract: We demonstrate longwave infrared (LWIR) generation with an optical parametric oscillator (OPO) based on quasi-phasematched orientation-patterned gallium arsenide (OPGaAs). The OPGaAs OPO was directly pumped with a Q-switched λ=2.054 μm Tm,Ho:YLF laser. OPGaAs samples representing three different grating periods were used to explore the LWIR OPO performance yielding outputs ranging from λ=2.5-2.7 μm (signal) and λ=8.8-11.5 μm (idler). Slope efficiencies for the combined signal and idler outputs reach as high as 26% while slope efficiencies for only the idler reached 8%. Spectral measurements of OPO output confirm good agreement with theoretical calculations.

***OCIS codes*:** (190.0190) Nonlinear optics; (190.4400) Nonlinear optics, materials; (190.4410) Nonlinear optics, parametric processes; (190.4970) Parametric oscillators and amplifiers

References and links

1. R. D. Peterson, D. Whelan, D. Bliss, and C. Lynch, "Improved material quality and OPO performance in OPGaAs," Proc. SPIE **7197**, 1-8 (2009).
2. P. Schunemann, L. Pomeranz, Y. Young, L. Mohnkern, and A. Vera, "Recent Advances in All-Epitaxial Growth and Properties of Orientation-Patterned Gallium Arsenide (OP-GaAs)," in Conference on Lasers and Electro-Optics/International Quantum Electronics Conference, OSA Technical Digest (CD) (Optical Society of America, 2009), paper CWJ5.
3. T. Skauli, K. L. Vodopyanov, T. J. Pinguet, A. Schober, O. Levi, L. A. Eyres, M. M. Fejer, J. S. Harris, B. Gerard, L. Becouarn, E. Lallier, and G. Arisholm, "Measurement of the nonlinear coefficient of orientation-patterned GaAs and demonstration of highly efficient second-harmonic generation," Opt. Lett. **27**, 628-630 (2002).
4. W. L. Wolfe, and G. L. Zissis, "The Infrared Handbook-Revised Edition," Washington D.C. Office of Naval Research, Department of the Navy, (1993).
5. A. Szilagyi, A. Hordvik, and H. Schlossberg, "A quasi-phase-matching technique for efficient optical mixing and frequency doubling," J. Appl. Phys. **47**, 2025-2032 (1976).
6. L. A. Gordon, G. L. Woods, R. C. Eckardt, R. K. Route, R. S. Feigelson, M. M. Fejer, and R. L. Byer, "Diffusion bonded stacked GaAs for Quasi-phase matched Second-Harmonic Generation of a Carbon Dioxide laser," Electron. Lett. **29**, 1942-1944 (1993).
7. D. F. Bliss, C. Lynch, D. Weyburne, K. O'Hearn, and J.S. Bailey, "Epitaxial growth of thick GaAs on orientation-patterned wafers for nonlinear optical applications," J. Cryst. Growth **287**, 673–678 (2006).
8. C. Kieleck, A. Hildenbrand, M. Eichhorn, D. Faye, E. Lallier, B. Gerard, and S.D. Jackson, "OP-GaAs OPO Pumped by 2μm Q-switched Lasers: Tm;Ho:Silica Fiber Laser and Ho:YAG Laser," Proc. of SPIE **7836**, (2010).
9. O. Levi, T.J. Pingeut, T. Skauli, L. A. Eyres, K. R. Parameswaran, J. S. Harris, Jr., M. M. Fejer, T. J. Kulp, S. E. Bisson, B. Gerard, E. Lallier, and L. Becouarn, "Difference frequency generation of 8-μm radiation in orientation-patterned GaAs," Opt. Lett. **27**, 2091-2093 (2002).
10. K. L. Vodopyanov, O. Levi, P. S. Kuo, T. J. Pinguet, J. S. Harris, M. M. Fejer, B. Gerard, L. Becouarn, and E. Lallier, "Optical parametric oscillator based on microstructured GaAs," Proc. SPIE **5620**, 63 (2004).
11. W. C. Hurlbut, Yun-Shik. Lee, K. L. Vodopyanov, P. S. Kuo, and M. M. Fejer, "Multiphoton absorption and nonlinear refraction of GaAs in the mid-infrared," Opt. Lett. **32**, 668-670 (2007).

12. T. Skauli, P. S. Kuo, K. L. Vodopyanov, T. J. Pinguet, O. Levi, L. A. Eyres, J. S. Harris, and M. M. Fejer, "Improved dispersion relations for GaAs and applications to nonlinear optics," J. of Appl. Phys., **94**, 6447-6455 (2003).

1. Introduction

Improvements in the quality of epitaxially grown orientation-pattern gallium arsenide (OPGaAs) [1,2] have made it an exceptional material for quasi-phasematched (QPM) nonlinear devices such as optical parametric oscillators (OPOs) in the 2-5 μm spectral region. OPGaAs is also attractive material for generating tunable radiation in the 8-12 μm atmospheric transmission region, due to its broad transparency (0.9-17 μm), high second-order nonlinear susceptibility (d_{14} ~94 pm/V) [3], high thermal conductivity (0.5 W $cm^{-1}K^{-1}$) [4], and high damage threshold. Tunable coherent LWIR sources are desirable for a variety of civilian and military applications, including molecular spectroscopy, remote sensing, and trace gas detection.

The principal alternative sources in this spectral region are CO_2 lasers, which are limited to discrete tuning, and lack the simplicity and compact size of solid-state systems; and nonlinear frequency conversion in birefringent crystals such as $ZnGeP_2$, which experience beam walkoff and detrimental thermal effects. OPGaAs avoids these problems, and can be designed to operate at any wavelength within its transparency range.

GaAs is optically isotropic, precluding the use of birefringent phasematching, and requiring the use of QPM for nonlinear frequency conversion. QPM spatially modulates the nonlinear properties of a given material where nonlinear interactions must obey conservation of energy and momentum. OPOs based on OPGaAs offer broad spectral coverage by transferring the energy from well-developed pump sources into the longer wavelength regions of interest.

Epitaxially grown OPGaAs eliminates problems encountered in the earliest demonstrations of QPM in this material [5,6], notably scattering losses from domain interfaces and labor-intensive processing to meet the necessary tolerances. Samples are fabricated in a two-step process, starting with molecular beam epitaxy (MBE) for growth of a template with desired periodic structure, followed by hydride vapor phase epitaxy (HVPE) for the bulk of the crystal growth [7]. A major advantage this approach is the flexibility of fabricating multiple structures on a single substrate.

Numerous devices based on OPGaAs have already been demonstrated [1,2,8-10], including difference frequency generation (DFG) at 8 μm [9]. Broad tuning has been demonstrated in an OPGaAs OPO pumped by a tunable PPLN OPO, with output tunable from λ=2-11.1 μm range [10]. A major constraint on the design of OPGaAs-based devices is that strong two-photon absorption [11] limits the pumping of OPGaAs devices to sources with wavelengths longer than approximately λ=1.8 μm. When generating longer wavelength idlers, using a longer wavelength pump source reduces the quantum defect in going from the pump wavelength to the desired longwave IR output. OPOs based on PPLN or similar materials can provide the necessary pump wavelengths for an OPGaAs-based device, but add the complexity of a second frequency conversion stage to the overall system, and typically require line-narrowing to meet the spectral acceptance bandwidth of OPGaAs. Direct 2 μm sources, like the Tm,Ho:YLF laser, are preferable for their relative simplicity, and inherently narrow (~1.5 nm) linewidth that is well within the OPGaAs acceptance bandwidth. In this paper, we investigate the performance of OPGaAs for the generation of longwave infrared output, when pumped by a direct laser source operating at 2 μm.

2. Experimental

The experimental setup is shown in Fig. 1. The pump source was a diode-pumped cryogenically cooled Tm,Ho:YLF laser (λ=2.054 μm, 500 Hz, 4 mJ) with a pump spectral

linewidth of approximately 1.5 nm. The pump was attenuated to ~0.6 J/cm^2 (760 μJ) to stay below the ~1 J/cm^2 damage threshold of the OPGaAs crystal coatings. To control the incident power intensity without changing other beam parameters, an attenuator consisting of a halfwave plate and polarizer was used. A Faraday isolator was inserted to prevent backreflections into the pump cavity. A second halfwave plate was used to vary the pump polarization incident on the OPO cavity. The pump propagated through the OPGaAs crystal in the $[\bar{1}10]$ crystal direction while the polarization at the entrance face was along the [001] crystal plane. The pump beam was focused into the crystal to a 1/e^2 radius of 200 μm and OPO the cavity length was kept relatively small (~1.9 cm) to minimize threshold. Samples, listed in Table 1, each had one of three different grating periods: Λ=76 μm, 82 μm, and 84 μm. These were all grown in the same HVPE run, cut to a length of 15.4 cm, polished, and antireflection-coated at λ=1.98-2.1 μm, λ=2.5-2.85 μm, and λ=7.8-8.85 μm. (Note that the thickness listed includes a substrate thickness of 0.5 mm.)

Table 1: OPGaAs samples with dimensions and QPM period

Sample	QPM Period (μm)	Dimensions (mm)		
		Length	Width	Thickness
26	76	15.4	6.5	1.4
29	82	15.4	7.0	1.4
27	84	15.4	6.4	1.4
28	84	15.4	6.5	1.4

We investigated two different cavity geometries: (1) a standard SRO cavity resonating the signal; and (2) an asymmetric cavity in which the input mirror was highly reflective at idler, and the outcoupler highly reflective at signal, causing signal and idler to exit from opposite ends of the cavity (by convention the shorter wavelength output is the signal while the longer wavelength output is the idler). The design of the asymmetric cavity was intended to suppress backconversion and support only pump to signal and idler conversion. By removing the two output wavelengths at opposite ends of the cavity, the signal and idler waves remaining in the cavity are largely counterpropagating, limiting phasematching of the reverse process. Since this also lowers the overall resonant intensity, it leads to lower efficiency in the forward conversion process as well. Backconversion still may occur for sufficiently high pumping levels, but pump energy is limited by the damage threshold of the antireflective coatings on the crystal. Both cavities double-passed the pump to increase conversion efficiency, and in fact used the same outcoupling mirror. A dichroic mirror that passes the pump and reflects the signal was used to collect the signal transmitted by the input mirror in the asymmetric configuration.

For spectral analysis, an extended-range InGaAs detector was chosen to detect signal output while a cryogenically cooled HgCdTe detector, which covers the entire expected idler range, was chosen to measure the idlers. These two detectors were used in conjunction with a Horiba Triax 320 1/3m spectrometer using a 100 g/mm grating and Stanford Research Systems lock-in amplifier to collect the output spectrum from each sample. High-pass and low-pass filters were used to isolate the signal and idler in order to measure output power and the beam propagation factor or beam quality factor, M^2, independently. All of the M^2 measurements were completed by knife edge scan in both the x and y directions and qualitative images were captured using a Electrophysics PV-320 camera.

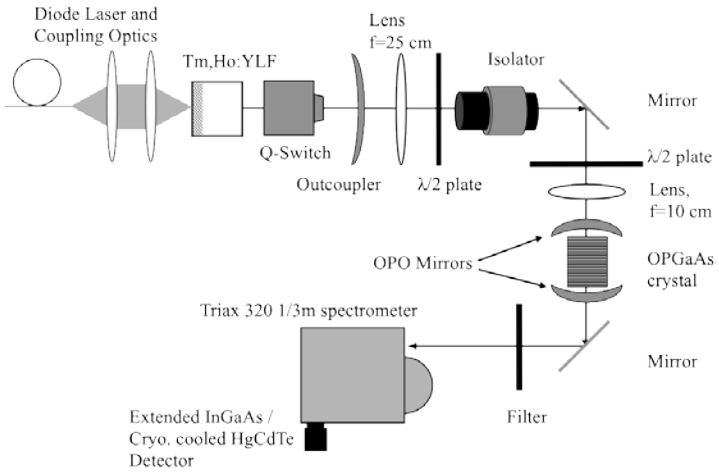

Fig. 1: OPGaAs OPO experimental setup

3. Results

Fig. 2 shows the performance of each sample in the SRO and asymmetric cavities. Slope efficiencies in the SRO cavity range from 2-8% for idler only, and 13-26% for signal and idler combined. These values are slightly lower than our previously reported midwave infrared (MWIR) OPGaAs OPO results [1] but the midwave experiments used a doubly-resonant oscillator, operated much closer to degeneracy, and used more recently grown OPGAs material. The asymmetric cavity yields idler slope efficiencies ranging from only 1-4%, with slope efficiencies of 2-12% for combined signal and idler. This is substantially lower than the SRO case with higher thresholds as well. These results were not unexpected given that neither the signal nor the idler truly resonates within the cavity. In order to obtain comparable output from the asymmetric cavity, it may be enough to pump it at higher energies, but with the damage threshold of 1 J/cm^2, this would risk damage to the coatings on the OPGaAs samples. It may be possible, however, to modify the signal and idler reflectivites in the asymmetric cavity to optimize the OPO output while still retaining its unbalanced nature. Additionally, in both cavities, samples with the two longer grating periods have a slightly poorer performance than the shortest period sample, likely due to the signal and idler pair operating further from degeneracy, along with variations in the anti-reflection coatings and cavity mirrors toward the extremes of the operating range.

Output from the SRO cavity begins to experience rollover starting around 400 μJ of pump energy, an effect usually attributed to backconversion or thermal effects. In the asymmetric cavity rollover is not observed and the output increases with pumping in the expected linear fashion. Observing the temporal behavior of residual pump pulses should indicate whether or not backconversion is occurring within either OPO.

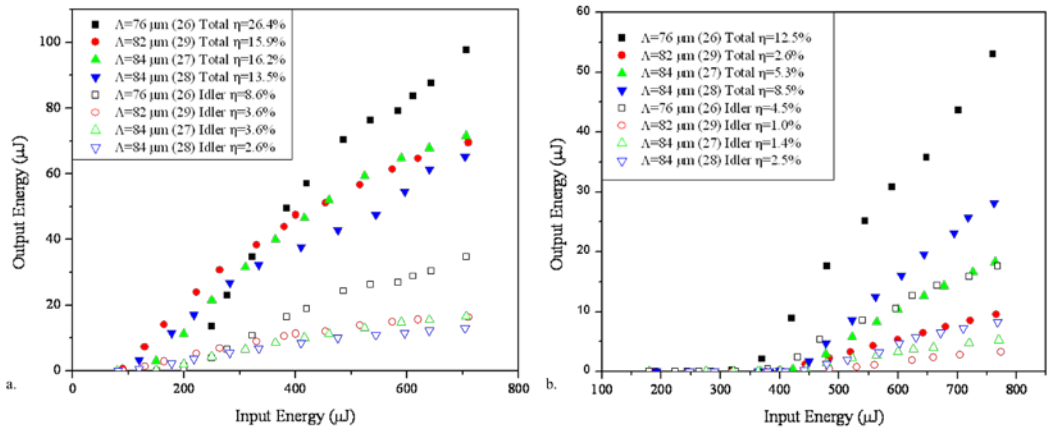

Fig. 2: OPO performance for SRO cavity (a) and asymmetric cavity (b) showing both idler and total output. Sample number is in parentheses and slope efficiency is listed in plot. (Signal and idler wavelengths are: 2.7 μm, 8.8 μm [Λ=76 μm]; 2.55 μm, 10.7 μm [Λ=82 μm]; 2.5 μm, 11.5 μm [Λ=84 μm]).

Fig. 3 compares residual pump profiles of the Λ=76 μm sample in both the SRO and asymmetric cavities, at various pump energies. The undepleted pump profile was obtained by misaligning one of the OPO mirrors in order to ensure that no pump to signal and idler conversion took place. In the SRO cavity, backconversion in the pump profile emerges by a pump energy ≥ 500 μJ. Still, a significant amount of conversion is apparent in the profile when compared to the undepleted pump. The point at which backconversion become noticeable in the pump profiles correspond roughly to the pump energy at which rollover begins in the performance plots. We can therefore conclude that backconversion of the pump is contributing to output rollover. In contrast, the pump pulses profiles from the asymmetric cavity show no indications of backconversion, as expected, based on the cavity design. On the other hand, we can see that far less conversion of the pump is occurring overall, which corresponds to the poorer performance of the cavity. Temporal profiles of the pump, signal, and idler pulses from the Λ=76 μm sample in the SRO cavity at an input energy of 500 μJ are shown in Fig. 4.

The asymmetric cavity was designed to suppress backconversion and it did accomplish this but at the expense of limiting output. Even with backconversion present, the SRO cavity provided greater output and remained the more effective cavity configuration. For this reason remaining characterization of the LWIR OPGaAs OPO relied on the SRO cavity.

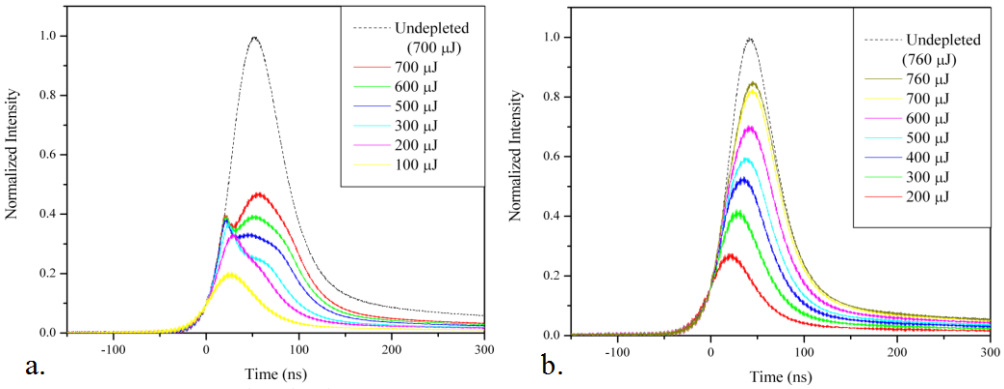

Fig. 3: Pump profiles for the Λ=76 μm sample at increasing input pump energies in the SRO cavity (a) and the asymmetric cavity (b). Traces normalized to the undepleted pump profile.

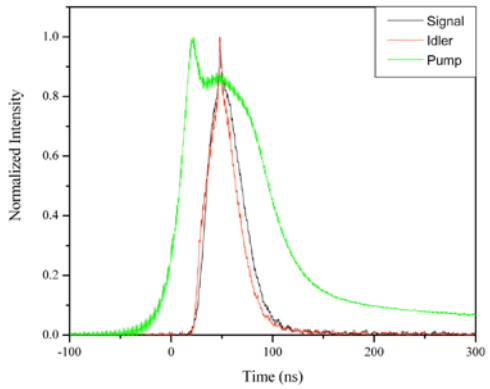

Fig. 4: Normalized pump, signal and idler profiles for the Λ=76 μm sample in the SRO cavity at a pump energy of 500 μJ.

Fig. 5 shows the signal and idler spectra from each QPM period, and a comparison of these measured values with theoretical calculations based on [12]. The measured peak wavelengths demonstrated good agreement with the theoretical tuning curve for GaAs pumped by a λ=2.054 μm source at room temperature. Table 2 lists the expected and measured signal and idler pair for each sample. These measurements were all made with the crystals at room temperature. The spectra from the SRO and asymmetric cavities were qualitatively the same.

Table 2: Calculated and measured signal and idler wavelengths for each OPGaAs sample

Sample	Period (μm)	Calculated Signal (μm)	Measured Signal (μm)	Calculate Idler (μm)	Measured Idler (μm)
25	76	2.679	2.673	8.751	8.805
29	82	2.540	2.540	10.649	10.689
27	84	2.505	2.497	11.451	11.460
28	84	2.505	2.497	11.451	11.505

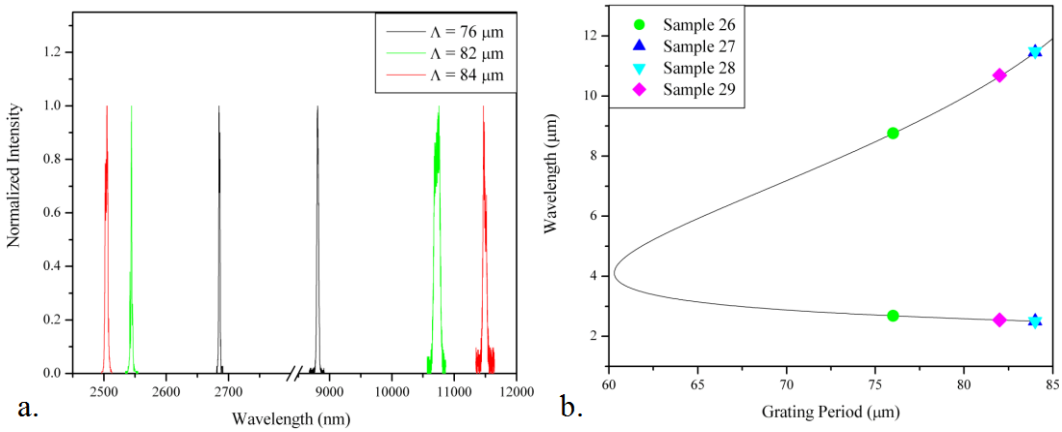

Fig. 5: Signal and idler spectra for each OPGaAs grating period (a); OPGaAs OPO tuning data for 2 μm pump, where solid line shows calculated tuning curve based on [12] (b).

Fig. 6 shows M^2 measurements for the signal and idler pair from the sample with the Λ=76 μm. Both signal and idler outputs demonstrate near diffraction-limited beam quality with M^2s ≈1.2, not entirely expected given the much larger resonant mode size for the idler, and the relatively modest aperture of the OPGaAs crystal. Good idler beam quality is attributed to the diffraction-limited quality of the Tm,Ho:YLF pump laser. Since the idler is not resonating within the SRO cavity, its beam characteristics are defined by the pump source rather than cavity. While the x and y directions for the idler appear to focus to the same point, the signal appears to be quite astigmatic. Similar astigmatism was seen in other samples as well.

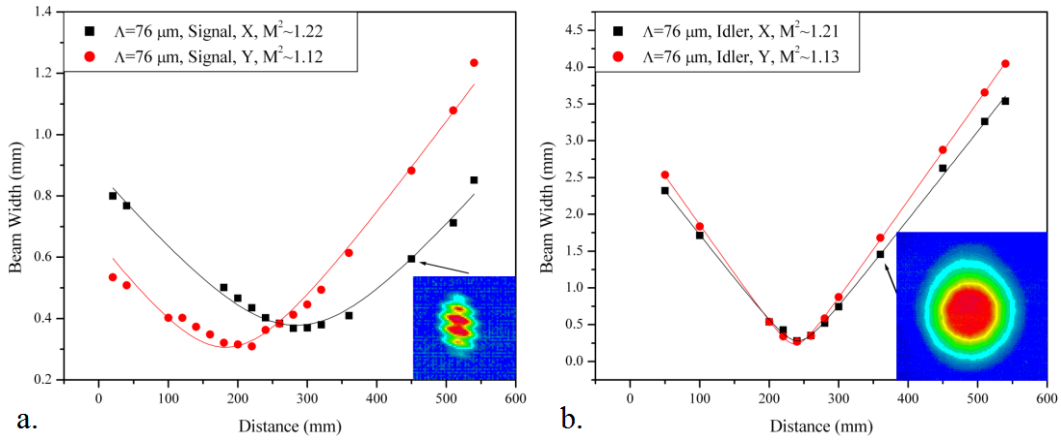

Fig. 6: M^2 measurement for signal at λ=2.67 μm (a) and idler at λ=8.8 μm (b) in the x and y directions for OPGaAs with the Λ=76 μm sample. (Insets show camera images of each beam.)

4. Conclusion

We have demonstrated LWIR generation in an OPGaAs OPO using direct laser pumping by a Tm,Ho:YLF laser operating at λ=2.054 μm. OPO designs typically aim to obtain the greatest amount of output, with reasonable conversion efficiency and modest pump threshold. Backconversion reduces the overall amount of signal and idler retrieved from an OPO and in

OPGaAs appears to be as significant an issue as thermal effects, if not more so. The asymmetric cavity described above was designed to avoid backconversion and succeed in this respect but at the cost of lower output and conversion efficiency and higher threshold. By these measures, the standard SRO cavity performed far better, despite the presence of backconversion at higher pump energies. Pumping the asymmetric cavity harder is limited by the damage of the OPGaAs damage threshold. Different mirror reflectivity, however, might allow the asymmetric cavity to reach higher outputs. With the SRO configuration, the longwave OPGaAs OPO demonstrated slope efficiencies approaching 30%, and a respectable beam quality with M^2 values roughly 1.2 for both signal and idler. Spectral data additionally confirm the validity of OPGaAs dispersion relations into the longwave spectral region.